

NANOSTRUCTURE OF THE PENETRATION DEPTH IN Nb CAVITIES: DEBUNKING THE MYTHS AND NEW FINDINGS

Y. Trenikhina*, A. Romanenko, Fermilab, Batavia, USA
J. Kwon, J.-M. Zuo, MatSE, UIUC, Urbana, United States

Abstract

Nanoscale defect structure within the magnetic penetration depth of 100nm is key to the performance limitations of niobium superconducting radio frequency (SRF) cavities. Using a unique combination of advanced thermometry during cavity RF measurements, and TEM structural and compositional characterization of the samples extracted from cavity walls at both room and cryogenic temperatures, we directly discover the existence of nanoscale hydrides in SRF cavities limited by high field Q-slope, and show the decreased hydride formation after 120C baking. Crucially, in extended studies, we demonstrate that adding 800C hydrogen degassing - both with AND without light BCP afterwards - restores the hydride formation to the pre-120C bake level correlating perfectly with the observed high field Q-slope behavior. We also show absence of niobium oxides along the grain boundaries and the modifications of the surface oxide upon 120C bake, which contradicts some of the widely used models of the niobium surface.

INTRODUCTION

High Field Q-slope (HFQS) is an outstanding degradation effect which significantly limits performance of niobium SRF cavities. The characteristic signature of HFQS is a rapid decrease of the quality factor (Q) values starting from accelerating gradients of ≈ 25 MV/m. Temperature mapping of the cavities during the RF measurements demonstrates strongly dissipating localized regions to be the cause of HFQS onset. Strong dissipation of those regions stems from a sudden increase in the surface resistance, causing Joule heating of the Nb near-surface. Characterization of intrinsic features of Nb near-surface that are responsible for the increased dissipation, is crucial for understanding HFQS.

Electropolishing (EP), buffered chemical polishing (BCP), and even annealing at 800C with no further chemical treatments, result in cavity performance limited by HFQS. Only mild 120°C baking of Nb fine grain cavities for 12 hours eliminates HFQS. A decade of HFQS research revealed a few potential hypotheses, but failed to find a complete explanation of HFQS and its cure, satisfying all experimental findings. The most recent promising model is based on the formation of lossy niobium nanohydrides in the penetration depth [1]. Nanohydrides may remain superconducting due to the proximity effect up to the breakdown field, which is determined by their size. The model attributes HFQS onset field to such a loss of proximity-induced superconductivity, which manifests as a strong increase in residual resistance and causes HFQS. The presence of a high concentration of

interstitial hydrogen in the penetration depth, upon cooling to 2K, may coalesce into lumps of niobium hydrides. A challenging part is that in order to search for such nanohydrides directly, cryo-investigations at < 100 K are required as at room temperature no hydrides are present.

Our studies are based on a unique combination of advanced thermometry during cavity RF measurements, and TEM structural and compositional characterization of the samples extracted from cavity walls at both room and cryogenic temperatures. In order to directly correlate different dissipation characteristics with surface nanostructure and to determine the underlying mechanisms of HFQS in Nb SRF cavities, we base our studies on the comparison of cutouts from cavities with and without HFQS, similar to previous studies [2–4]. Comparison of the original cavity cutouts with known heating profiles guarantees the absence of artifacts associated with witness sample preparation.

In this work we present structural and analytic comparison of cross-sectional samples taken from the cavities with and without HFQS. TEM diffraction techniques were performed at room and cryogenic (94K) temperatures. Temperature dependent nano-area electron diffraction (NED) and scanning electron nano-area diffraction (SEND) reveal the formation of stoichiometric, non-superconducting, small niobium hydride inclusions. Mild baking is shown to decrease nanohydride sizes and/or density, which directly correlates with the observed suppression of the high field Q-slope in SRF cavities. Additionally, high resolution TEM (HRTEM) and bright field (BF) imaging show similar surface oxide thickness and lack of any oxidation along grain boundaries. Electron energy loss spectroscopy (EELS) chemical characterization of the surface oxides suggests slight oxygen enrichment just below the oxides after the mild bake.

EXPERIMENTAL METHODS

Preparation of Cavities Cutouts

Our studies are based on the comparison of cutouts from cavities with and without HFQS. Two Nb fine grain ($\approx 50 \mu\text{m}$) TESLA shape cavities with resonant frequency $f_0 = 1.3$ GHz were used. Both cavities were electropolished, and one of them was additionally baked at 120°C for 48 hours. Dependence of the quality factor on peak surface magnetic field at 2 K was measured for both cavities, and both also had temperature maps acquired during rf measurements in order to identify the regions for cutout. As expected, the EP-only cavity that had no final mild bake showed prominent HFQS, while the performance of the EP+120°C baked cavity was free from HFQS.

* yuliatr@fnal.gov

Temperature maps of both cavities recorded at $E_{\text{acc}} = 28$ MV/m, which is above the HFQS onset field, are shown in Fig. 1. The unbaked cavity shows large regions of elevated temperature (up to 0.4 K) as compared to the cavity that was baked at 120°C , which had no such extended dissipative regions. Based on the temperature maps, samples with characteristic rf field dependences for each of the treatments (shown in Fig. 2) were cut out from both cavities. The selected characteristic sample from the unbaked cavity (labeled “EP” for the following) shows a drastic increase of the local temperature as the surface rf field amplitude reaches about 100 mT.

This is in contrast with the characteristic cutout from the 120°C baked cavity (labeled “EP120C” for the following), which shows no such feature. Cutouts were of circular shape with 11 mm diameter and were extracted from the cavities by an automated milling machine with pure water used as a lubricant.

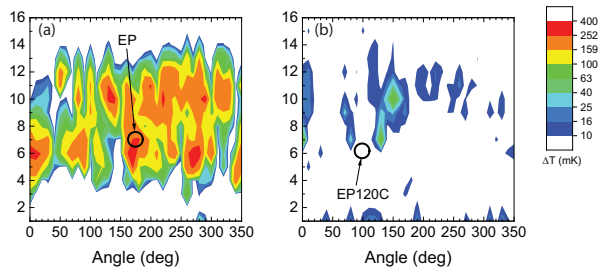


Figure 1: Temperature maps at $E_{\text{acc}} = 28$ MV/m of: (a) unbaked EP cavity, (b) EP+ 120°C baked cavity. Locations of the cutout samples are marked by black circles.

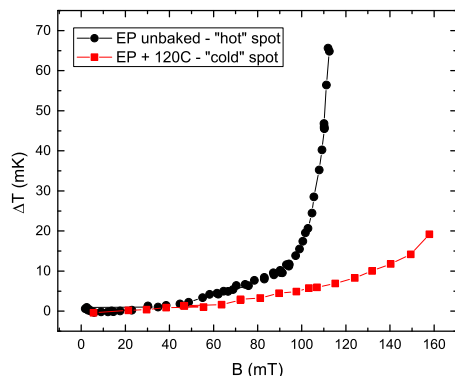


Figure 2: Dissipation characteristics at different rf field amplitudes of EP and EP120C spots.

Additionally, one further cutout from the unbaked cavity was subjected to 800°C vacuum degassing for 3 hours, and $20\ \mu\text{m}$ buffered chemical polishing (labeled “EP800C-BCP” for the following). One flat Nb sample from Nb sheet was EP and baked at 800°C for 3 hours (labeled “EP800C” for the following).

Characterization of Cavities Cutouts

Cross sectional TEM samples were prepared from the cavity cutouts by the Focused Ion Beam (FIB) lift-out technique. Two types of TEMs were used for this work: field-emission gun (FEG) TEM and thermionic LaB₆ gun TEM. The key difference between these two microscopes is the higher brightness of FEG relative to the thermionic LaB₆ gun. Brightness, which defines the electron dose in a small probe, is a crucial parameter for the investigation of dose-sensitive niobium nanohydrides. The details of the sample preparation as well as description of the TEM techniques that were used for this work can be found in [5]. A Gatan liquid nitrogen cooled double-tilt stage was used for the low temperature measurements. FIB-prepared cavity cutout samples were cooled to 94 K inside the TEM for approximately 30 min. An additional 30 min was allowed before the measurements for temperature stabilization.

TEMPERATURE-DEPENDENT STRUCTURAL INVESTIGATIONS

Room Temperature Measurements

Room temperature TEM phase characterization was first acquired on all of the samples in order to investigate the state of the Nb-H system in the warm state. NED patterns were taken with a probe size of approximately 80 nm in diameter. Areas located directly underneath the niobium oxides, as well as areas a few hundred nanometers deep, were explored (Fig. 3). Similar diffraction patterns produced by body centered cubic (BCC) niobium with no additional ordered stoichiometric phases were found on all the samples we investigated. Thus TEM electron diffraction shows that hydrogen behaves like a lattice gas and occupies random tetrahedral interstitial sites in Nb at room temperature. This phase is called solid solution (α -phase).

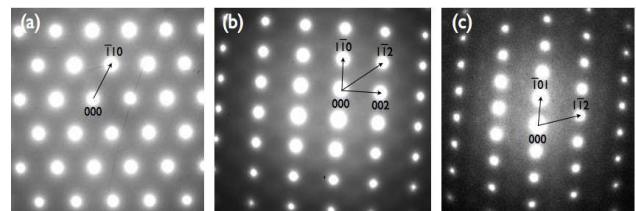


Figure 3: Room temperature NED for EP and EP120C cutouts: (a) Nb [111] zone axis, (b) Nb [110] zone axis, (c) Nb [131] zone axis.

Cryogenic Temperature Measurements

Prior to TEM measurements, the possibility of niobium hydride precipitation in the cutouts from the same cavities was explored in the optical cryogenic stage of a confocal microscope. Using the same experimental setup, evidence of large Q disease-causing hydrides was demonstrated in the previous study. No evidence of Nb hydrides precipitation was observed in the cutouts with the spatial resolution of the confocal microscope ($\approx 1\ \mu\text{m}$).

Cryogenic temperature phase characterization of all samples (EP, EP120C, EP800C-BCP and EP800C) was accomplished with SEND in the thermionic gun TEM. EP and EP120C samples were additionally characterized with NED in FEG TEM. Fig. 4 shows a SEND map taken from the EP sample along with a TEM image of the sample at 94K. NED patterns were taken automatically in a sequential manner from the Nb near-surface region which was imaged prior to scanning. Every square in Fig. 4a represents a sample area of diameter equal to the diameter of the diffraction probe.

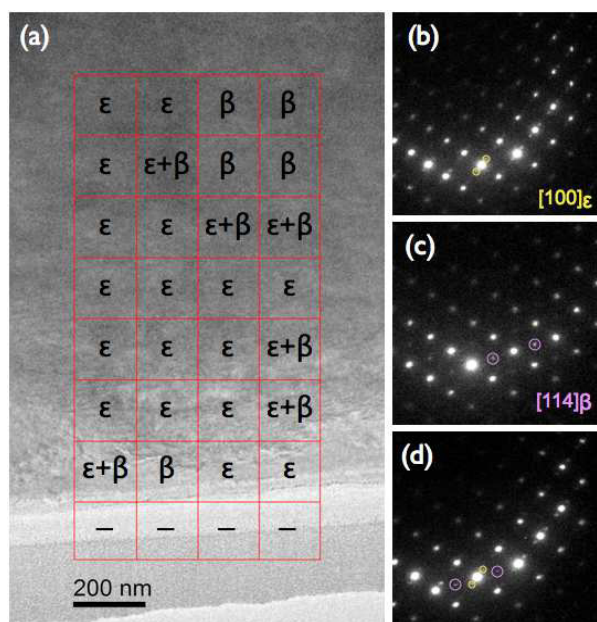


Figure 4: a) SEND map of EP sample at 94 K using LaB₆ TEM, (b) ϵ -phase Nb₄H₃ overlapped with Nb, (c) β -phase NbH overlapped with Nb, (d) ϵ - and β -phases overlapped with Nb.

Fig. 4b-d show NED representative patterns taken from the EP sample. “Half-order” additional reflections are clearly visible along with reflections from Nb matrix. Orientation of Nb crystal is close to [110] zone axis. Two niobium hydride phases were found in EP sample at 94K.

Fig. 4b shows a ϵ -phase niobium hydride diffraction pattern overlapped with [110] Nb. ϵ -phase was recognized by “half-order” reflections along the [110]_{cubic} direction [6], [7]. The orientation of observed ϵ -phase domains is close to the [114] Nb₄H₃ zone axis.

Fig. 4c shows a β -phase niobium hydride diffraction pattern overlapped with [110] Nb. β -phase was recognized by reflections at $(\frac{1}{2} \frac{1}{2} 1)$ _{cubic} in terms of cubic BCC Nb reflections [8]. The orientation of β -phase domains is close to the [100] NbH zone axis.

SEND mapping of EP120C sample at 94K demonstrated only BCC Nb diffraction pattern with no additional reflections. One EP sample and one EP120C sample were evaluated by SEND at 94K.

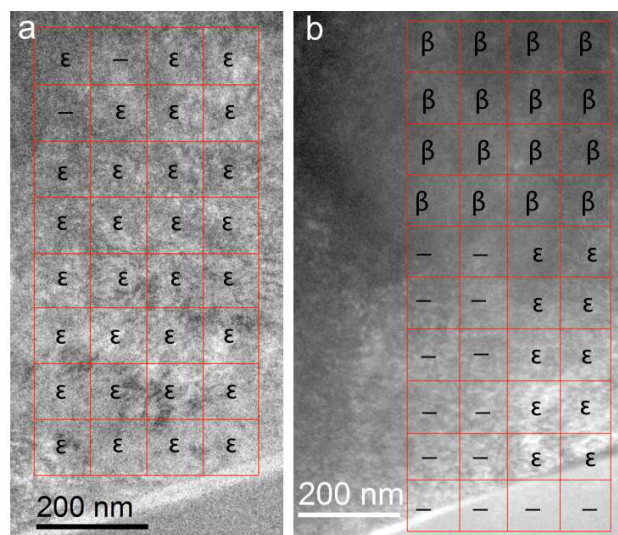


Figure 5: (a) SEND map of EP800C sample at 94 K, (b) SEND map of EP800C-BCP sample at 94 K.

SEND maps of EP800C and EP800C-BCP sample were taken at 94K. Diffraction maps of both samples (Fig. 5) show the presence of the same low temperature niobium hydride phases (ϵ and β) as for the unbaked cavity sample.

Additional NED structural characterization of the EP and EP120C samples was performed in FEG TEM at 94 K. In order to collect diffraction patterns from the near-surface area, the NED probe was positioned by the deflection coils onto the TEM sample for each exposure. The size of the NED probe was approximately 80 nm. NED diffraction patterns were collected by sequentially moving the probe along the length of the sample. Fig. 6 (a)-(c) and (d)-(f) show typical cryogenic temperature NED patterns taken from EP and EP120C samples, respectively. Additional second phase reflections are clearly observed along with Nb matrix reflections at 94 K in both types of samples. Additional low temperature reflections in EP samples are more intense and frequent than additional reflections in EP120C samples. Comparing EP and EP120C samples, the number of probed spots exhibiting reflections of an additional low-temperature phase differ as shown in Fig. 7. For the EP samples, 68% of probed spots showed additional reflections, whereas for the EP120C samples, 27% of the probed spots showed additional reflections. Three FIB prepared EP and three EP120C samples were investigated with NED.

Despite the NED in FEG TEM shows second phase precipitants at low temperature in both types of samples, indexing of the additional reflections was not possible. Most of the detected second phase reflections were not in compliance with any reported phase of niobium hydride. This can be explained in terms of dissociation of the native low temperature niobium hydride phases under the electron beam exposure. It has been noticed that additional low-temperature reflections rapidly vanish under exposure to the electron beam. Heating of the exposed area by electron bombardment or

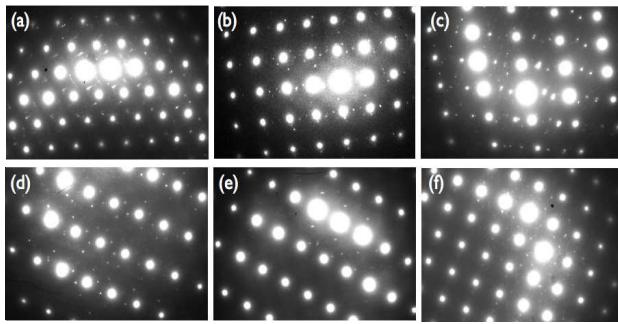


Figure 6: a)-(c) Diffraction patterns taken from EP samples at 94K; (d)-(f) Diffraction patterns taken from EP120C sample at 94K.

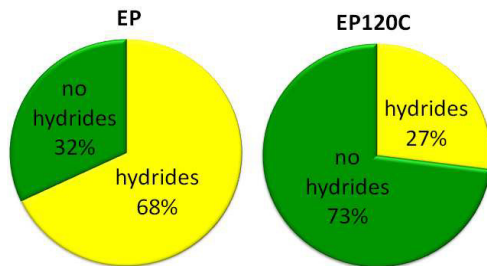


Figure 7: Fraction of area with and without NED-detected hydrides in EP and EP120C samples.

direct electron energy transfer allows hydrogen to regain its mobility and move to different parts of the sample, which can lead to severe distortion and dissociation of niobium hydrides.

Discussion

SEND and NED structural investigations directly show precipitation of niobium hydrides at cryogenic temperatures. SEND mapping shows that appearance of low temperature precipitants in Nb near-surface correlates perfectly with HFQS-limited cavity performance. The significantly lower area affected by nanohydride precipitation in EP120C cutouts found by the near-surface NED investigations is consistent with the hydride precipitation suppression by the 120°C bake, as proposed recently in [2,9]. At this stage, it is not yet possible to definitively say if it is the volume density or the size of the nanohydrides which is affected. However, the removal of the HFQS suggests that it is likely the size.

Reappearance of high nanohydride population after additional 800°C vacuum treatment for 3 hours, with and without 20 μm buffered chemical polishing, suggests hydrogen reabsorption in the furnace during cool down and BCP.

GRAIN BOUNDARIES AND SURFACE OXIDES

TEM Imaging and Spectroscopy

HRTEM imaging and EELS were used for detailed imaging and comparison of the surface oxides and grain bound-

aries in EP120C and EP samples. The appearance of an approximately 5 nm-thick amorphous oxide layer (Nb_2O_5) in HRTEM images is similar for both types of samples (Fig. 8).

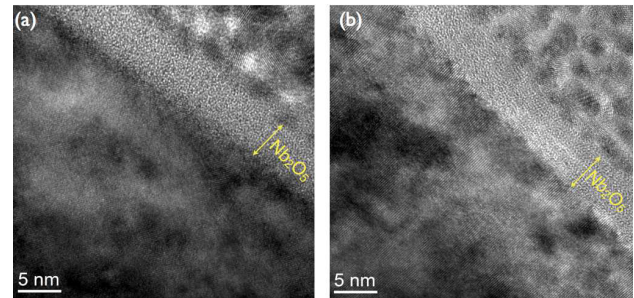


Figure 8: a) HRTEM image of EP120C sample; (b) HRTEM image of EP sample.

Several samples with uniformly thin grain boundary regions were prepared from the cavity cutouts. Images of the grain boundaries in the EP and EP120C spot samples are represented in Fig. 9. HRTEM images of the cavity cutouts do not show an amorphous contrast from the isolating niobium pentoxide along the grain boundaries, in contradiction to some literature models [10].

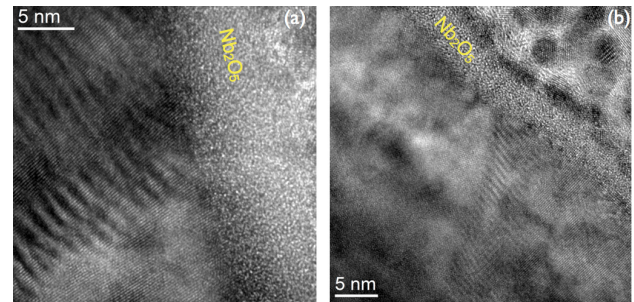


Figure 9: (a) EP120C sample; (b) EP sample.

EELS investigations of the surface oxides in the EP120C and EP samples were performed as a way to make detailed comparisons of niobium valence across the oxide layer. Fig. 10a shows EELS spectra for niobium $M_{2,3}$ edge. EELS spectra were taken for the four regions marked in the STEM image of the niobium near surface (Fig. 10b). The $M_{2,3}$ edge of niobium is the result of the transition of Nb 3p electrons to unoccupied Nb 4d and 5s states. Spin-orbit coupling of the 3p orbital causes the appearance of two peaks (M_2 and M_3). All niobium core loss spectra were calibrated with respect to carbon K-edge onset at 286 eV using the second derivative method [11]. Three spectra for each region were added after the background subtraction with log-polynomial function [12]. Thickness of the sample in the region of interest was estimated to be 41 nm from the Log-Ratio Method [11].

The linear relationship between the chemical shift of M-edge onset and niobium valence can be used to determine the niobium oxidation state [13]. For both samples, the $M_{2,3}$

Table 1: Experimental Position of Nb M₃ Peak in Different Regions for EP120C and EP Samples

Sample	Region 1	Region 2	Region 3	Region 4	Shift
EP	366.7	367.2	367.5	367.8	1.1
EP120C	366.8	368.0	367.9	368.3	1.5

peak for each region shows a clear chemical shift toward higher energy as a function of distance from the Nb metallic surface. The EP120C sample shows a greater shift than the EP sample. The observed shifts for both the EP and EP120C samples agree well with previous results of Tao et al [13].

Table 1 summarizes the positions of M₃ peaks for both samples for each region. The last column shows the difference in position from region 1 to region 4. The M₂ peaks follow the same trend as the M₃ peaks. The comparatively larger shifts of the M_{2,3} peaks of the EP120C sample is an indication of higher niobium valence in each region relative to that in the EP sample. This suggests inward (toward the bulk of Nb) oxygen diffusion during the mild bake. According to X-ray investigations of Nb/Nb-oxide interfaces [14], an increase of *x* for NbO_{*x*} underneath Nb₂O₅ in EP120C sample can be caused by the enrichment in interstitial oxygen.

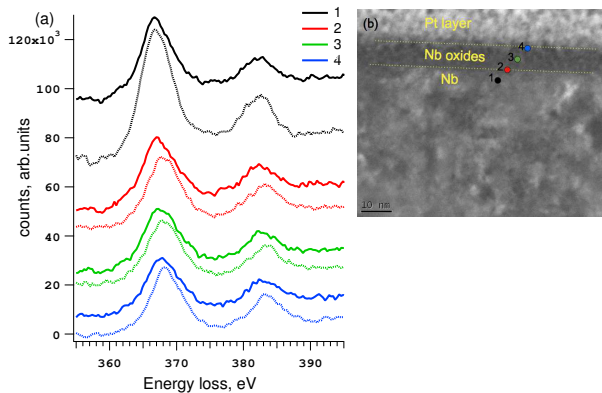


Figure 10: (a) EELS taken from EP (solid line) and EP120C (dashed line); (b) STEM image indicating the regions where the EELS spectra were taken from.

Discussion

It was discussed in the past that niobium oxide structure may also get modified during the 120°C bake in several different ways [14–17]. Our investigations show that amorphous Nb₂O₅ of about 5 nm thick is very similar in both EP and EP120C cutouts. The slightly increased niobium oxidation state in EP120C is consistent with the increased oxygen concentration right underneath the oxide, as found before [14, 16]. This increased oxygen concentration may be a reason for the ~1-2 nΩ higher residual resistance in 120°C baked cavities, which can be restored to the pre-120°C bake level by a hydrofluoric acid rinse [18] since the oxygen-rich layer gets converted to the newly grown oxide.

Finally, a very important finding is the lack of insulating Nb₂O₅ along grain boundaries. This contradicts a model

of the niobium surface, frequently used up to now, which suggests the presence of oxidized grain boundaries, crack corrosion, and isolated niobium suboxides islands [19].

CONCLUSION

Microscopic comparison of the original cutouts from SRF cavities with and without HFQS was performed in order to identify the underlying cause of the HFQS and the mechanism of its cure. NED and SEND revealed the presence of nanoscale niobium hydride precipitants in the near-surface of the cavity cutouts at cryogenic temperature for the first time. The area affected by low temperature precipitants and/or their size correlates perfectly with HFQS-limited cavity performance after EP and 800°C bake with and without further BCP material removal. Mild 120°C bake was demonstrated to reduce the amount of and/or change the distribution of niobium hydrides in the near-surface layer. Phase identification in SEND demonstrated the presence of β- and ε-niobium hydrides in the EP and 800°C-baked EP cutouts at 94K.

Comparison of the grain boundaries and surface oxides in the cavities with and without HFQS were conducted with HRTEM imaging and EELS in order to investigate any possible differences. HRTEM investigation of grain boundaries showed no niobium pentoxide along the grain boundaries and a similar structure of grain boundaries in EP and EP120C samples. Identical thickness of the surface niobium pentoxide was found from HRTEM images of the EP and EP120C cutouts. EELS chemical characterization of the niobium oxidation state as a function of distance from the surface revealed that EP120C samples have higher chemical shifts for all regions. EELS characterization confirms inward oxygen diffusion from the oxide into the bulk, coherently with the hydrofluoric acid rinse beneficial effect observed on 120°C baked cavities.

REFERENCES

- [1] A. Romanenko, F. Barkov, L. D. Cooley, A. Grassellino, Supercond. Sci.Tech. 26, 035003 (2013).
- [2] A. Romanenko, L.V. Goncharova, Supercond. Sci. Tech. 24, 105017 (2011).
- [3] A. Romanenko, A. Grassellino, F. Barkov, A. Suter, Z. Salman, T. Prokscha, Appl. Phys. Lett. 104, 072601 (2014).
- [4] A. Romanenko, C. J. Edwardson, P. G. Coleman, P. J. Simpson, Appl. Phys. Lett. 102, 232601 (2013).
- [5] Y. Trenikhina, A. Romanenko, J. Kwon, J.-M. Zuo, J.F. Zasadzinski, J. Appl. Phys. 117 (15), 154507 (2015).
- [6] V. Somenkov, S. Shil’stein, Progress in Materials Science 24, 267 (1980).
- [7] B. Makenas, H. Birnbaum, Acta Metallurgica 30, 469 (1982).

- [8] T. Schober, M. Pick, H. Wenzl, *Physica Status Solidi (A) Applied Research* 18, 175 (1973).
- [9] A. Romanenko, F. Barkov, L. D. Cooley, A. Grassellino, *Supercond. Sci. Tech.* 26, 035003 (2013).
- [10] J. Halbritter, *Journal of The Less-Common Metals* 139, 133 (1988).
- [11] R. F. Egerton, *Electron energy-loss spectroscopy in the electron microscope*, (New York: Springer, 2011).
- [12] D. Bach, H. Störmer, R. Schneider, D. Gerthsen, J. Verbeeck, *Microscopy and Microanalysis* 12, 416 (2006).
- [13] R. Tao, R. Todorovic, J. Liu, R. J. Meyer, A. Arnold, W. Walkosz, P. Zapol, A. Romanenko, L. D. Cooley, R. F. Klie, *J. Appl. Phys.* 110, 124313 (2011).
- [14] M. Delheusy, A. Stierle, N. Kasper, R. P. Kurta, A. Vlad, H. Dosch, C. Antoine, A. Resta, E. Lundgren, J. Andersen, *Appl. Phys. Lett.* 92, 101911 (2008).
- [15] C. Benvenuti, S. Calatroni, V. Ruzinov, "Diffusion of oxygen in niobium during bake-out", *Proceedings of the 10th Workshop on RF Superconductivity*, Tsukuba, Japan (2001).
- [16] I. Arfaoui, C. Guillot, J. Cousty, C. Antoine, *J. Appl. Phys.* 91 (11), 9319 (2002).
- [17] Q. Ma, R. A. Rosenberg, *Appl. Surf. Sci.* 206, 209 (2003).
- [18] A. Romanenko, A. Grassellino, F. Barkov, J. P. Ozelis, *Phys. Rev. ST Accel. Beams* 16, 012001 (2013).
- [19] J. Halbritter, *Proceedings of the 10th Workshop on RF Superconductivity*, Tsukuba, Japan (2001).